Engineering 6 (2020) 1006–1012

Contents lists available at ScienceDirect

Engineering

journal homepage: www.elsevier.com/locate/eng

Research
Energetic Materials and Interdisciplinary Science—Article

Construction of an Unusual Two-Dimensional Layered Structure for Fused-Ring Energetic Materials with High Energy and Good Stability

Yongan Feng [a,b], Mucong Deng [b], Siwei Song [b], Sitong Chen [b], Qinghua Zhang [b,*], Jean'ne M. Shreeve [a,*]

[a] Department of Chemistry, University of Idaho, Moscow, ID 83844-2343, USA
[b] Institute of Chemical Materials, China Academy of Engineering Physics, Mianyang 621900, China

ARTICLE INFO

Article history:
Received 28 September 2019
Revised 29 November 2019
Accepted 8 January 2020
Available online 10 June 2020

Keywords:
Energetic materials
Fused heterocycles
2D layered structure
High energy
Stability
Sensitivity

ABSTRACT

The creation of high-performance energetic materials with good mechanical sensitivities has been a great challenge over the past decades, since such materials have huge amounts of energy and are thus essentially unstable. Here, we report on a promising fused-ring energetic material with an unusual two-dimensional (2D) structure, 4-nitro-7-azido-pyrazol-[3,4-*d*]-1,2,3-triazine-2-oxide (NAPTO), whose unique 2D structure has been confirmed by single-crystal X-ray diffraction. Experimental studies show that this novel energetic compound has remarkably high energy (detonation velocity D = 9.12 km·s^{-1}; detonation pressure P = 35.1 GPa), excellent sensitivities toward external stimuli (impact sensitivity IS = 18 J; friction sensitivity FS = 325 N; electrostatic discharge sensitivity EDS = 0.32 J) and a high thermal decomposition temperature (203.2 °C), thus possessing the dual advantages of high energy and low mechanical sensitivities. To our knowledge, NAPTO is the first fused-ring energetic material with 2D layered crystal stacking. The stabilization mechanism toward external stimuli were investigated using molecular simulations, and the theoretical calculation results demonstrate that the ultraflat 2D layered structure can buffer external mechanical stimuli more effectively than other structures by converting the mechanical energy acting on the material into layer sliding and compression. Our study reveals the great promise of the fused-ring 2D layered structure for creating advanced energetic materials.

1. Introduction

Energetic materials (EMs)—a family of special energy materials that can quickly release huge amounts of chemical energy—have substantially contributed to the progress of human civilization and social development since Alfred Nobel first tamed nitroglycerin in 1863 [1,2]. Numerous EMs based on a diverse range of backbones, such as alkanes, cyclanes, aromatics, strain-caged heterocycles, and nitrogen-heterocycles, have been synthesized over the past decades (Fig. 1(a)) [3–20]. However, EMs with very huge energy generally encounter the problem of poor stability toward external stimuli (e.g., impact, friction, electrostatic spark, and heat), and thus lack the safety like 2,4,6-trinitrotoluene (TNT) or 1,3,5-triamino-2,4,6-trinitro benzene (TATB). This makes most EMs dangerous to produce, handle, and use in military and civilian applications [21]. The newly reported 2,4,6-triamino-5-nitropyrimidine-1,3-dioxide (ICM-102) may be a good insensitive high explosive, but its strong interaction with water molecules hinders its further application (the dehydration temperature of ICM-102 is as high as 178 °C) [22]. Recently, scientists have turned their attention to fused-ring energetic compounds due to the conjugated structures and good molecular stability of these substances; examples of these compounds include 2,9-dinitroditriazolo[1,5-*d*:5′,1′-*f*]-1,2,3,4-tetrazine (DNDTT), 1,2,9,10-tetranitrodipyrazolo[1,5-*d*:5′,1′-*f*]-1,2,3,4-tetrazine (TNDPT), and 3,6-dinitropyrazolo[4,3-*c*]pyrazole-1,4-diamine (DNPPDA) (Fig. 1(a)) [23–31]. Most of these compounds show good thermal stability and excellent energy performance, but their instability toward mechanical stimuli have not been completely resolved. Searching for powerful EMs with good safety remains a significant challenge.

Two-dimensional (2D) layered structures are generally considered to be effective "energy converters" that can transform the mechanical energy acting on bulk material into relative motion between layers when the material is subjected to intense

* Corresponding authors.
E-mail addresses: qinghuazhang@caep.cn (Q. Zhang), jshreeve@uidaho.edu (J.M. Shreeve).

https://doi.org/10.1016/j.eng.2020.01.013
2095-8099/

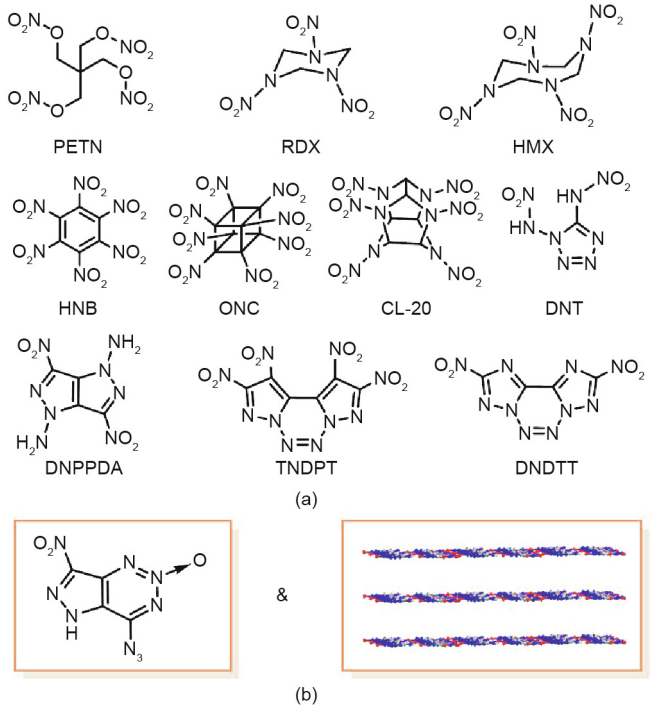

Fig. 1. (a) Various high-performance EMs based on diverse backbones; (b) a fused-ring EM with a 2D layered structure, as reported in this work. PETN: pentaerythritol tetranitrate; RDX: cyclotrimethylene trinitramine; HMX: cyclotetramethylene tetranitramine; HNB: hexanitrobenzene; ONC: octanitrocubane; CL-20: hexanitrohexaazaisowurtzitane; DNT: 1,5-di(nitramino)tetrazole; DNPPDA: 3,6-dinitropyrazolo[4,3-*c*]pyrazole-1,4-diamine; TNDPT: 1,2,9,10-tetranitrodipyrazolo[1,5-*d*:5′,1′-*f*]-1,2,3,4-tetrazine; DNDTT: 2,9-dinitroditriazolo[1,5-*d*:5′,1′-*f*]-1,2,3,4-tetrazine.

mechanical stimuli. This enables many lamellar materials (e.g., graphite, MoS_2, and h-BN) to be good solid lubricants in critical engineering applications [32–36]. In addition, theoretical studies have demonstrated that 2D layered structures can convert the mechanical energy acting on explosive materials into intermolecular interaction energy via the sliding and compression of the layers, thereby avoiding possible decomposition or detonation of high explosives [37–41]. Clearly, a 2D structure is preferable for the design of EMs. The insensitive high explosive TATB is a very good example. However, the energy density of TATB is relatively low; for example, the detonation energy of TATB is approximately 65% of that of the widely used cyclotetramethylene tetranitramine (HMX) [42]. Therefore, through the rational design of highly energetic fused compounds, the "energy converter" function of 2D structures could effectively stabilize the powerful fused-ring EMs, in order to achieve many new high-performance EMs with high energy, good thermal stability, and excellent mechanical sensitivities. Unfortunately, fused-ring EMs with a 2D layered structure have not been reported so far.

Herein, we report the design, synthesis, and characterization of the first fused-ring energetic compound with a 2D layered structure (Fig. 1(b)): 4-nitro-7-azido-pyrazol-[3,4-*d*]-1,2,3-triazine-2-oxide (NAPTO). X-ray single-crystal diffraction shows that the 2D planes in its crystal structure are constructed through hydrogen bonding and dipole–dipole interactions. The experimental results demonstrate that the as-synthesized NAPTO not only exhibits high detonation energy (comparable to that of HMX), but also owns good mechanical sensitivities (close to those of TNT) and good thermal stability, thus demonstrating the advantage of 2D fused structures in constructing high-performance EMs with good mechanical sensitivities.

2. Results and discussion

2.1. Design and synthesis of NAPTO

Although fused-ring EMs are under intense scrutiny by energetic materials experts, designing such substances with 2D layered structures still presents great challenges. Very recently, a primary explosive with an energy equivalent to that of HMX—that is, 6-nitro-7-azido-pyrazol[3,4-*d*]-1,2,3-triazine-2-oxide (ICM-103) was reported by our group [43]. Its extremely high sensitivity to mechanical stimuli can be partly attributed to its mixing π–π stacking mode. After checking the molecular structure of ICM-103 carefully, we found that the nitro (NO_2) and azide (N_3) groups in ICM-103 have partial negative charge and positive charge, respectively, while the N→O and N–H groups are potential hydrogen bond (HB) acceptors and HB donors, respectively. If the NO_2 and NH groups change places with each other, a 2D layered structure may be constructed due to the formation of a "cross-shaped" configuration of two sets of intermolecular interactions (HBs and dipole–dipole interactions), just like that of TATB (Fig. 2), resulting in good mechanical sensitivities. In addition, the NO_2 and the N_3 in NAPTO will be located on different sides of the parent ring, which will increase the stability of the molecule. This idea was later confirmed theoretically, and theoretical calculations showed that this newly designed NAPTO has a long-sought-after 2D structure (Section S1 in Appendix A).

Accordingly, NAPTO was synthesized using an approach that was more complicated than that of ICM-103 (Fig. 3). 4-Amino-3-cyanopyrazole (Compound 1 in the Fig. 3) was first synthesized according to reported methods [44,45]. Compound 2 was synthesized with a moderate yield of 67 wt% through the reaction of sodium azide and 4-amino-3-cyanpyrazole in dimethylformamide (DMF) using dimethylamine hydrochloride as the catalyst. Afterward, by treating Compound 2 with a mixture of fuming HNO_3 and 98% H_2SO_4 at 0–5 °C for 2 h, and then heating to 50 °C for 4 h, a clear orange-red solution was obtained. The dilute solution was extracted with ethyl acetate, and then brown crystals of NAPTO were obtained from the ethyl acetate by slow evaporation (Section S2 in Appendix A).

2.2. Crystal structure

The structure of NAPTO was fully characterized by infrared spectrum (IR), nuclear magnetic resonance (NMR), and elemental analysis (Section S2 in Appendix A). The accurate structure of NAPTO was confirmed by single-crystal X-ray diffraction. The detailed crystallographic data and refinement can be found in Section S3 in Appendix A. NAPTO crystallized in the orthorhombic space group *Pnma* with four molecules per unit cell. All the involved atoms in NAPTO, including the H atom and the NO_2, N_3,

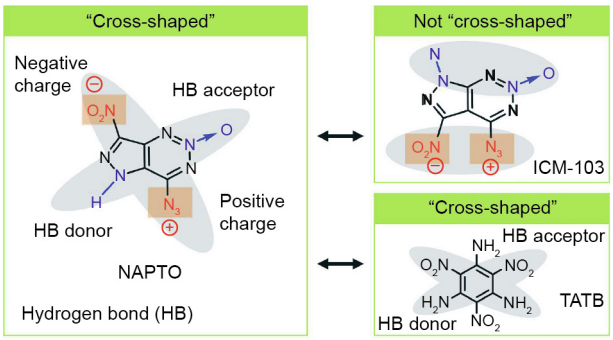

Fig. 2. The design and "cross-shaped" configuration of NAPTO.

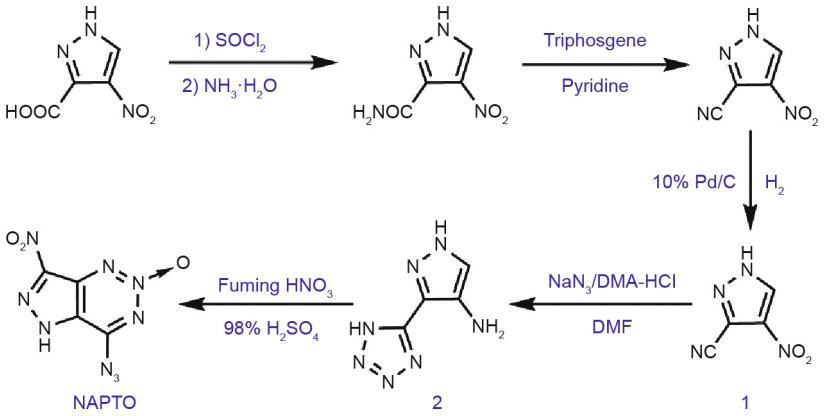

Fig. 3. The synthesis of NAPTO. DMA: dimethylamine.

and N→O groups, are accurately located in a plane, exhibiting a completely planar molecular configuration, of which the planarity surpasses those of known fused-ring EMs.

In the crystal structure, each molecule is connected to two neighboring molecules through HBs O1–H9–N9 and N4–H9–N9 with distances of 1.93 and 2.57 Å, respectively, forming an infinitely extended one-dimensional (1D) chain (Fig. 4). The adjacent chains are further self-assembled into 2D planes via dipole–dipole interactions between the O atoms of the nitro group (NO_2) and N atoms of the triazo group (N_3) with a bond length of 2.781 Å (Fig. 4). As is known, the NO_2 group possesses a partially negative charge due to its strong electron-withdrawing characteristic. Previous studies have demonstrated that the N_3 group possesses a partially positive charge [11], which enables the N_3 group to strongly attract the negatively charged NO_2 group, forming a strong dipole–dipole interaction. Subsequently, the 2D planes are π-stacked layer by layer along the [010] direction into a graphite-like supramolecular structure (Fig. 4). As a result, NAPTO exhibits layer-by-layer π–π stacking—that is, an ultraflat 2D layered structure—possessing a possible "energy converter" advantage over those of reported traditional EM (HMX, octanitrocubane (ONC), hexanitrohexaazaisowurtzitane (CL-20), hexanitrobenzene (HNB)) and fused EMs (DNDTT, TNDPT, DNPPDA). The layer spacing of NAPTO was measured to be 2.855 Å, indicating a tighter π–π stacking. In addition, NAPTO had a high crystal density (1.852 $g·cm^{-3}$), which is consistent with the predicted density (> 1.80 $g·cm^{-3}$, Section S1 in Appendix A), satisfying the requirement of high explosives (≥ 1.78 $g·cm^{-3}$) [40,41].

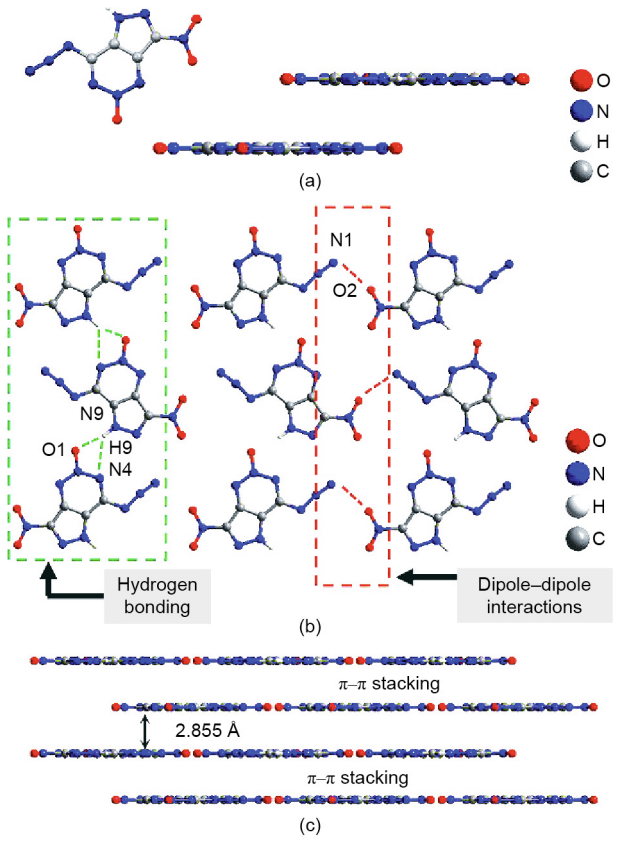

Fig. 4. (a) Crystal structure and ultraflat molecular configuration of NAPTO; (b) intermolecular interactions in the layers of the NAPTO crystal; (c) three-dimensional (3D) structure of NAPTO based on π–π interaction.

2.3. Energy

Energy level is the most critical property for EMs because it determines their efficiency. The energy properties of EMs are usually represented by two important detonation parameters, detonation velocity (D) and detonation pressure (P), both of which, according to the classical C-J equation, are mainly determined by the density and heat of formation [46–48]. The heat of formation can be obtained by using the Gaussian09 (revision D.01) suite of programs based on high-precision theoretical methods (Section S4 in Appendix A). As shown in Table 1, the solid-phase heat of formation of NAPTO is positive and was calculated to be 3.47 $kJ·g^{-1}$, which is significantly higher than those of traditional EMs such as TNT (0.24 $kJ·g^{-1}$), cyclotrimethylene trinitramine (RDX) (0.34 $kJ·g^{-1}$), and HMX (0.35 $kJ·g^{-1}$). Furthermore, NAPTO shows a high density of 1.85 $g·cm^{-3}$ at 296 K, which is higher than that of the most widely used RDX (1.82 $g·cm^{-3}$) and close to that of HMX (1.89 $g·cm^{-3}$).

With the density and heat of formation values, the detonation performance of NAPTO was assessed using the EXPLO5 (Version 6.02, OZM Research, Czech Republic) program. As expected, NAPTO exhibited a high detonation performance, and the calculated D and P were 9.12 $km·s^{-1}$ and 35.1 GPa, respectively (Table 1), which surpass two of the most widely used EMs, TNT (7.45 $km·s^{-1}$, 23.5 GPa) and RDX (8.75 $km·s^{-1}$, 34.7 GPa). In particular, the D of NAPTO is comparable to that of HMX (9.10 $km·s^{-1}$), indicating that NAPTO possesses a high energy comparable to that of HMX. In other words, NAPTO is an excellent candidate for use as a high-performance EM, and its energy is on par with the most powerful EMs in use today.

Table 1
Physicochemical and energetic properties of several typical EMs and NAPTO.

Items	TNT	RDX	HMX	NAPTO
M (g·mol^{-1})	227.13	222.12	296.16	223.02
N (%)	18.50	37.84	37.84	56.50
Ω_{CO_2} (%)	−73.97	−21.61	−21.61	−39.44
ρ (g·cm^{-3})	1.65	1.82	1.89	1.85
$\Delta_f H_m$ (kJ·g^{-1})	0.24	0.34	0.35	3.47
D (km·s^{-1})	7.45	8.75	9.10	9.12
P (GPa)	23.5	34.7	39.0	35.1
IS (J)	15.0	7.5	7.0	18.0
FS (N)	353	120	112	325
EDS (mJ)	0.37	0.15	0.10	0.32
T_{dec} (°C)	240.0	204.5	275.0	203.2

M: formula weight; N: nitrogen content; Ω_{CO_2}: oxygen balance; ρ: crystal density; $\Delta_f H_m$: heat of formation; D: calculated detonation velocities; P: calculated detonation pressure; IS: impact sensitivity; FS: friction sensitivity; EDS: electrostatic discharge sensitivity; T_{dec}: decomposition temperature.

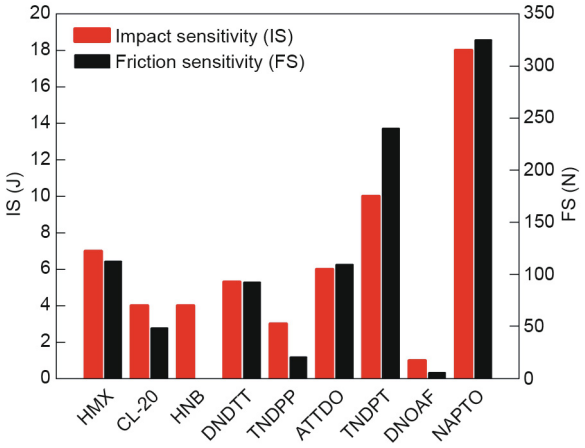

Fig. 5. Comparison of the impact and friction sensitivities of NAPTO and eight high-performance EMs ($D \geq 9.0$ km·s^{-1}).

2.4. Thermal stability

In addition to its high energy, the stability properties of NAPTO, including its thermal stability and mechanical sensitivity, are of particularly interest due to its 2D layered structure. Thermal stability is crucial to the safety of EMs because it reflects the difficulty of accidental combustion or explosion of EMs under an external thermal load. In general, a heat resistance above 180 °C is highly desirable for practical application [49]. However, in most cases, EMs with huge amounts of energy are thermodynamically unstable. Given that NAPTO showed a high energy density comparable to that of HMX, while isomer ICM-103 has a relatively low decomposition temperature, we were slightly concerned about the thermosensitive properties of NAPTO. Here, differential scanning calorimetry (DSC) and thermogravimetric (TG) analysis were used to assess the thermal stability of NAPTO (Section S6 in Appendix A). As shown in Fig. S9 in Appendix A, the thermal decomposition of NAPTO occurred at an onset temperature of 203.2 °C and a peak temperature of 214.2 °C, which is significantly higher than that of its isomer ICM-103 (160.3 °C), and is almost comparable to those of the two most powerful explosives, namely, RDX (204.5 °C) and CL-20 (195.0 °C) [30]. This demonstrates the good thermal stability of NAPTO for practical use. Compared with ICM-103, the 2D structure of NAPTO may play a critical role in its good thermal stability due to the strong hydrogen bonding and dipole–dipole interactions within the layers.

2.5. Sensitivities toward mechanical stimuli

Stability toward external stimuli, such as impact, friction, and electrostatic spark, is also crucial for EMs. Here, using Bundesanstalt für Materialforschung und -prüfung (BAM) methods, the mechanical sensitivities of NAPTO were tested (Section S7 in Appendix A); the results are summarized in Table 1. The measured impact, friction, and electrostatic spark sensitivities of NAPTO were 18.0 J, 325 N, and 0.32 J, respectively. As shown in Fig. 5, the sensitivities of NAPTO are much superior to those of reported EMs with a D higher than 9.0 km·s^{-1}, including traditional explosives (e.g., CL-20, ONC, 4,4-dinitroazoxyfurazan (DNOAF)) and new fused-ring explosives (e.g., DNDTT, 1,3,4,6-tetranitro-1,4-dihydro pyrazolo [4,3-*c*]pyrazole (TNDPP), 6-amino-tetrazolo[1,5-*b*] 1,2,4,5-tetrazine-4,7-*N*-dioxide (ATTDO), and TNDPT). It is clear that the mechanical sensitivities of NAPTO are better than those of HMX (7.0 J, 112 N, and 0.10 J), and are almost equivalent to those of TNT (15.0 J, 353 N, and 0.37 J). In other words, NAPTO not only exhibits an outstanding detonation energy comparable to that of HMX, but also has excellent mechanical-stimuli stability close to that of TNT. Considering that the energy of NAPTO (a secondary explosive) and ICM-103 (a primary explosive) are almost equal, but their mechanical sensitivities are significantly different (IS = 18.0 J and FS = 325 N vs IS = 4.0 J and FS = 60 N), we believe that this 2D structure has a significant role in improving the safety of explosives.

2.6. Stabilization mechanism

To gain insight into the stabilization mechanism of NAPTO, we investigated the nature of its ultraflat 2D layered structure in response to external mechanical stimuli using molecular simulations (Section S8 in Appendix A) [39].

As seen in Fig. 6, the following observations can be made: ① Sliding and compression of the layers occur in the NAPTO crystal when under a simulated external mechanical force; this causes a change in the interaction energy between adjacent layers (Figs. 6(a)–(c), (g), and (h)) without causing a chemical change, showing that the NAPTO crystal can absorb a certain amount of mechanical energy and thus prevent decomposition to a certain extent. Among the deformations, the sliding action can absorb a mechanical energy of 155.5 kJ·mol^{-1} (Fig. 6(c)), while the compression can absorb 60.7 kJ·mol^{-1} (Fig. 6(h)). This suggests that the desensitizing mechanism of an ultraflat 2D structure can be explained by energy dissipation due to the sliding and compression of the layers, in which layer sliding contributes approximately 72% of the energy dissipation capability. ② In layer sliding, the van der Waals (vdW) interactions have a variation magnitude of only 30.3 kJ·mol^{-1}, which is much less than that of the electrostatic interactions (144.0 kJ·mol^{-1}), implying that the electrostatic interactions have a greater influence on the total interaction energy. ③ As shown in Figs. 6(c) and (f), the total interlayer interaction energy of NAPTO varies from −38.0 to 117.5 kJ·mol^{-1} (a variation magnitude of 155.5 kJ·mol^{-1}). In comparison, the total interaction energy of TATB (an insensitive layered explosive with an energy of only 65% of HMX's energy) varies from −1.4 to 32.5 kJ·mol^{-1} (a variation magnitude of 33.9 kJ·mol^{-1}), indicating that NAPTO can absorb much more mechanical energy than TATB when under an external stimulus. That is, ultraflat structures have great potential to allow EMs to maintain good mechanical sensitivities at very high energy levels. This is consistent with the experimental results (Table 1) and has been further confirmed by the calculated sliding barrier (E_{Sb}, Fig. 6(g)), where the region of the E_{Sb} of NAPTO below 300 MJ·m^{-3} is smaller than that of TATB, but much larger than that of HMX [39].

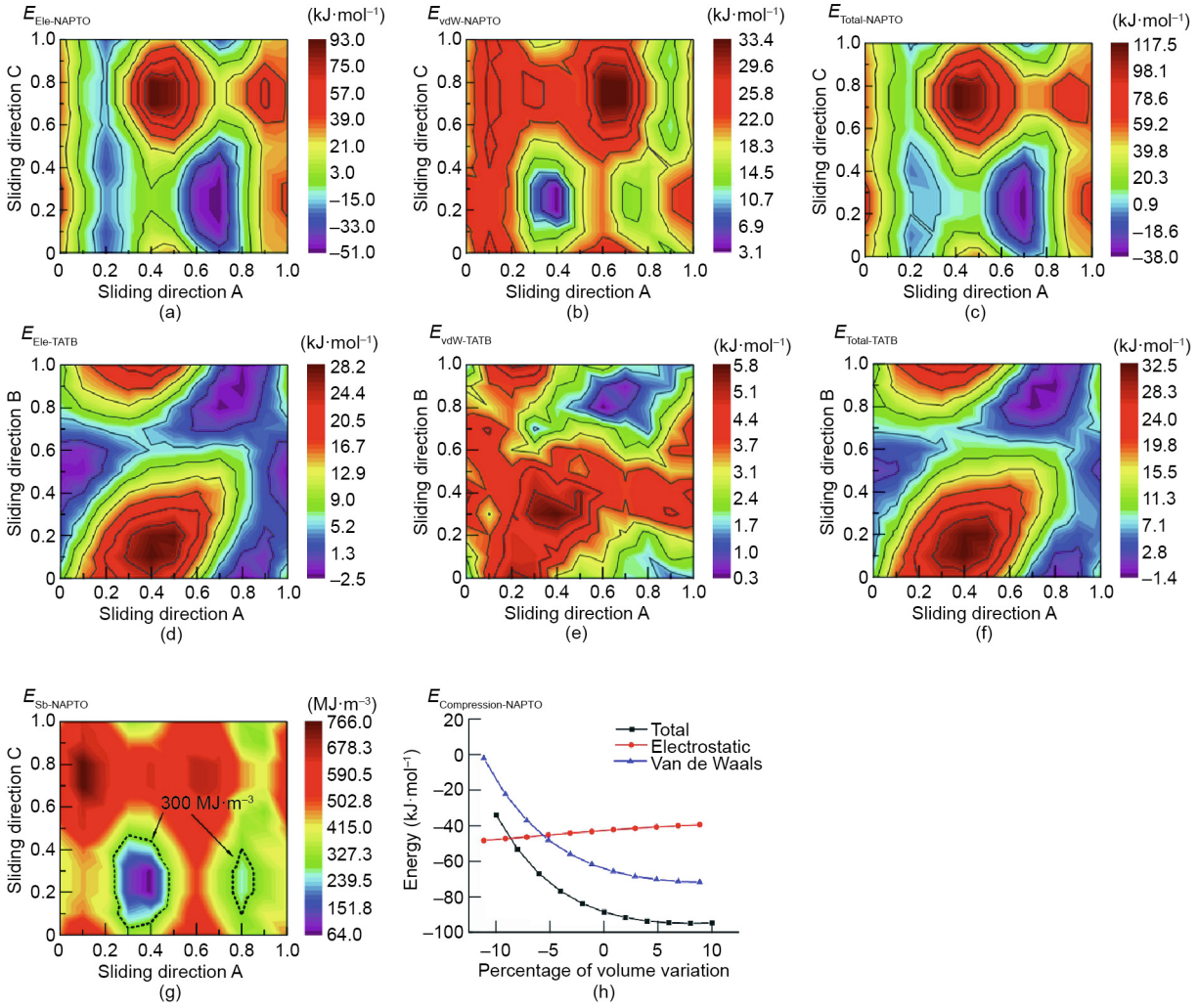

Fig. 6. (a), (b), and (c) show the electrostatic interaction energy ($E_{\text{Ele-NAPTO}}$), vdW interaction energy ($E_{\text{vdW-NAPTO}}$), and total interaction energy of NAPTO ($E_{\text{Total-NAPTO}}$), respectively (in kJ · mol^{-1}); (d), (e), and (f) show the electrostatic interaction energy ($E_{\text{Ele-TATB}}$), vdW interaction energy ($E_{\text{vdW-TATB}}$), and total interaction energy of TATB ($E_{\text{Total-TATB}}$), respectively (in kJ · mol^{-1}); (g) shows the sliding barrier of NAPTO ($E_{\text{Sb-NAPTO}}$, in MJ·m^{-3})); (h) show the compression energy of NAPTO ($E_{\text{Compression-NAPTO}}$, in kJ · mol^{-1}).

In order to gain further insight into the desensitizing mechanism, the Hirschfeld surface and the 2D fingerprint were used to study the intralayer interactions and interlayer interactions (Fig. 7). The shapes of the Hirschfeld surfaces and the distribution of the red dots on the surfaces are usually used to indicate the sliding and compression characteristics of 2D materials. A plate-like shape with red dots located along the surface edges is preferred, since it represents planar conjugated molecular structures, relatively strong intralayer intermolecular interactions, and weak interlayer intermolecular interactions. The structures with these characteristics are more favorable for sliding and compression, in theory.

Fig. 7(a) indicates that only EMs with an extensive amount of strong HBs have the above characteristics (e.g., TATB, 3,3′-diamino-4,4′-azofurazan (DAAzF), 1,1-diamino-2,2-dinitroethene (FOX-7), and 3,5-dinitropyrazine-2,6-diamine-1-oxide (LLM-105)), while the other EMs without HBs or containing only a few HBs do not have these characteristics (e.g., TNT, HMX, and CL-20). Therefore, we are surprised that NAPTO has a Hirschfeld surface similar to that of TATB, since it has only one hydrogen atom in its structure. With the help of the 2D-fingerprint plot (Fig. 7(b)), it can be seen that, although there are very few HBs, relatively strong interactions still exist within the crystal layers of NAPTO and rather weak interlayer intermolecular interactions exist between the layers. Here, among neighboring intralayer molecules, O···H, N···H, and N···O are the dominant intermolecular interactions. Their distances are 1.93, 2.57, and 2.78 Å, respectively; these are much shorter than the sums of the van der Waals radii for O + H (2.65 Å), N + H (2.70 Å), and N + O (3.17 Å), indicating strong intralayer intermolecular interactions. In addition, these interactions represent 45.4% of the total intermolecular interactions (Fig. 7(c)). Between layers, the dominant forces are the relatively weak π–π interactions of O···O, O···C (and C···O), and N···C (and N···C). These represent 24.2% of the total intermolecular interactions, which is significantly lower than that of the intralayer interactions (Fig. 7(c)). Based on the above interaction systems, rigid layers are formed via relatively strong intralayer interactions, which—along with the rather weak interlayer interactions—makes sliding and compression between layers possible.

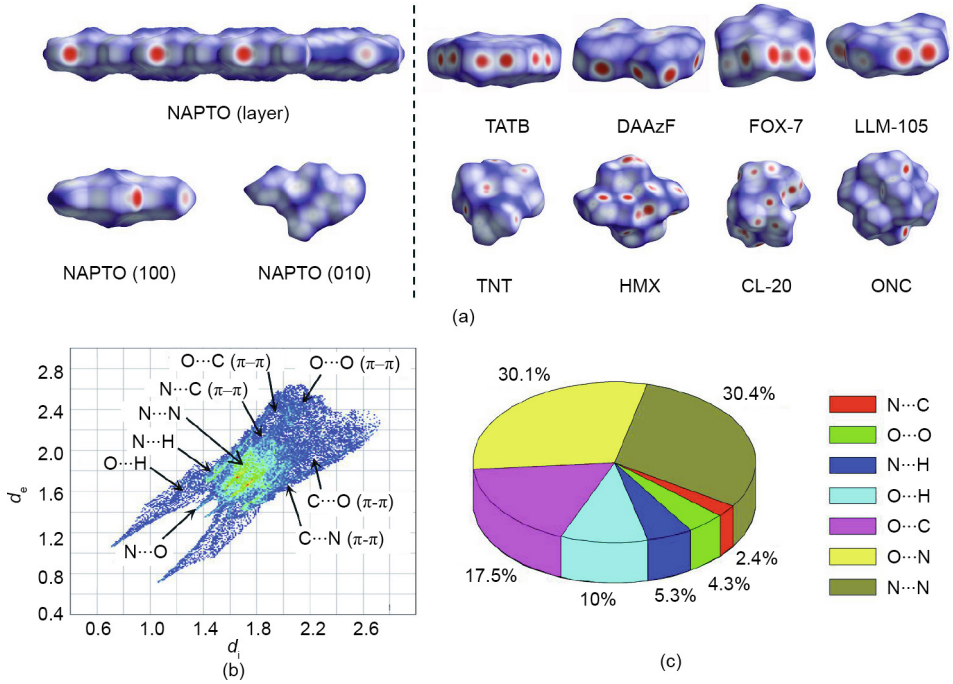

Fig. 7. (a) Hirschfeld surfaces of NAPTO, five low-energy explosives (TATB, DAAzF, FOX-7, LLM-105, and TNT) and three high-performance explosives (HMX, CL-20, and ONC); (b) 2D fingerprint plots in crystal stacking for NAPTO; (c) individual atomic contact percentage contributions to the Hirschfeld surface.

3. Conclusions

In conclusion, we demonstrate that the design and construction of the fused-ring 2D structure is a very powerful way to balance the contradicting energy and safety properties of EMs. By rearranging the energetic groups of an existing high-performance EM, we used HBs and dipole–dipole induction to create a promising graphite-like fused EM: NAPTO. Single-crystal X-ray diffraction showed that NAPTO exhibits an ultraflat 2D layered structure (tight π–π stacking between layers with a considerably short layer spacing of 2.883 Å), which is exceedingly rare in the field of EMs. NAPTO has a high detonation performance (D: 9.12 km·s^{-1} and P: 35.1 GPa), good thermal stability (203.3 °C), and desirable low mechanical sensitivity to external stimuli (IS: 18.0 J, FS: 325 N, and EDS: 0.32 J), as demonstrated by characterization with the EXPLO5 (v6.02) program, DSC-TG analysis, and the BAM method. A detailed computational study on the possible stabilization mechanism demonstrated that the 2D layered structure of NAPTO can effectively buffer against external stimuli, and thus balances the high energy and good mechanical sensitivities of NAPTO. In short, by making minor adjustments to the arrangement of the energetic groups (e.g., NO_2 and NH), the crystal packing of the energetic material has undergone significant changes (from mixing π–π stacking to 2D ultraflat stacking), which in turn has caused a huge difference in the macroscopic properties of the material (e.g., mechanical sensitivities and thermal stability). Our study demonstrates that the presented strategy of constructing a 2D fused-ring structure shows great promise for discovering new advanced EMs with a better balance between high energy and good stability.

Acknowledgements

Financial support from the Science Challenge Program (TZ2018004) and National Natural Science Foundation of China (21875228 and 21905258) is acknowledged.

Compliance with ethics guidelines

Yongan Feng, Mucong Deng, Siwei Song, Sitong Chen, Qinghua Zhang, Jean'ne M. Shreeve declare that they have no conflict of interest or financial conflicts to disclose.

Appendix A. Supplementary data

Supplementary data to this article can be found online at https://doi.org/10.1016/j.eng.2020.01.013.

References

[1] Klapötke TM. Structure and bonding: high energy density materials. Berlin: Springer; 2007. p. 36–7.
[2] Agrawal JP. High energy materials: propellants, explosives and pyrotechnics. Weinheim: Wiley-VCH Verlag GmbH & Co. KGaA; 2010. p. 1–2.
[3] Eiland PF, Pepinsky R. The crystal structure of cyclotetramethylene tetranitramine. Z Krist-Cryst Mater 1954;106(16):273–98.
[4] Choi CS, Prince E. The crystal structure of cyclotrimethylenetrinitramine. Acta Crystallogr B 1972;28(9):2857–62.
[5] Simpson RL, Urtiew PA, Ornellas DL, Moody GL, Scribner KJ, Hoffman DM. CL-20 performance exceeds that of HMX and its sensitivity is moderate. Propellants Explos Pyrotech 1997;22(5):249–55.
[6] Zhang MX, Eaton PE, Gilardi R. Hepta- and octanitrocubanes. Angew Chem Int Ed 2000;39(2):401–4.
[7] Eremets MI, Gavriliuk AG, Trojan IA, Dzivenko DA, Boehler R. Single-bonded cubic form of nitrogen. Nat Mater 2004;3(8):558–63.
[8] Zhurova EA, Stash AI, Tsirelson VG, Zhurov VV, Bartashevich EV, Potemkin VA, et al. Atoms-in-molecules study of intra- and intermolecular bonding in the pentaerythritol tetranitrate crystal. J Am Chem Soc 2006;128(45):14728–34.
[9] Zhurova EA, Zhurov VV, Pinkerton AA. Structure and bonding in β-HMX-characterization of a trans-annular N···N interaction. J Am Chem Soc 2007;129(45):13887–93.
[10] Joo YH, Shreeve JM. High-density energetic mono- or bis(oxy)-5-nitroiminotetrazoles. Angew Chem Int Ed 2010;49(40):7320–3.
[11] Klapötke TM, Martin FA, Stierstorfer J. C2N14: an energetic and highly sensitive binary azidotetrazole. Angew Chem Int Ed 2011;50(18):4227–9.
[12] Raza Z, Pickard CJ, Pinilla C, Saitta AM. High energy density mixed polymeric phase from carbon monoxide and nitrogen. Phys Rev Lett. 2013;111(23):235501.
[13] Fischer D, Klapotke TM, Stierstorfer J. 1,5-Di(nitramino)tetrazole: high sensitivity and superior explosive performance. Angew Chem Int Ed 2015;54(35):10299–302.

[14] Bennion JC, Chowdhury N, Kampf JW, Matzger AJ. Hydrogen peroxide solvates of 2,4,6,8,10,12-hexanitro-2,4,6,8,10,12-hexaazaisowurtzitane. Angew Chem Int Ed 2016;55(42):13118–21.
[15] Xia K, Sun J, Pickard CJ, Klug DD, Needs RJ. Ground state structure of high-energy-density polymeric carbon monoxide. Phys Rev B 2017;95:144102.
[16] Yu Q, Yin P, Zhang JH, He CL, Imler GH, Parrish DA, et al. Pushing the limits of oxygen balance in 1,3,4-oxadiazoles. J Am Chem Soc 2017;139(26):8816–9.
[17] Zhang WQ, Zhang JH, Deng MC, Qi XJ, Nie FD, Zhang QH. A promising high-energy-density material. Nat Commun 2017;8:1–7.
[18] Zhang C, Sun CG, Hu BC, Yu CM, Lu M. Synthesis and characterization of the pentazolate anion *cyclo*-N_5^- in $(N_5)_6(H_3O)_3(NH_4)_4Cl$. Science 2017;355(6323):374–6.
[19] Xu YG, Wang Q, Shen C, Lin QH, Wang PC, Lu M. A series of energetic metal pentazolate hydrates. Nature 2017;549(7670):78–81.
[20] Yang C, Zhang C, Zheng ZS, Jiang C, Luo J, Du Y, et al. Synthesis and characterization of cyclo-pentazolate salts of NH_4^+, NH_3OH^+, $N_2H_5^+$, $C(NH_2)_3^+$, and $N(CH_3)_4^+$. J Am Chem Soc 2018;140(48):16488–94.
[21] Zhang CY. Origins of the energy and safety of energetic materials and of the energy & safety contradiction. Propellants Explos Pyrotech 2018;43(9):855–6.
[22] Wang Y, Liu YJ, Song SW, Yang ZJ, Qi XJ, Wang KC, et al. Accelerating the discovery of insensitive high-energy-density materials by a materials genome approach. Nat Commun 2018;9(2444):1–11.
[23] Thottempudi V, Forohor F, Parrish DA, Shreeve JM. Tris(triazolo)benzene and its derivatives: high-density energetic materials. Angew Chem Int Ed 2012;51(39):9881–5.
[24] Chavez DE, Bottaro JC, Petrie M, Parrish DA. Synthesis and thermal behavior of a fused, tricyclic 1,2,3,4-tetrazine ring system. Angew Chem Int Ed 2015;54(44):12973–5.
[25] Klenov MS, Guskov AA, Anikin OV, Churakov AM, Strelenko YA, Fedyanin IV, et al. Synthesis of tetrazino-tetrazine 1,3,6,8-tetraoxide (TTTO). Angew Chem Int Ed 2016;55(38):11472–5.
[26] Yin P, Zhang JH, Mitchell LA, Parrish DA, Shreeve JM. 3,6-Dinitropyrazolo[4,3-*c*]pyrazole-based multipurpose energetic materials through versatile N-functionalization strategies. Angew Chem Int Ed 2016;55(41):12895–7.
[27] Thottempudi V, Yin P, Zhang JH, Parrish DA, Shreeve JM. 1,2,3-triazolo[4,5-*e*]furazano[3,4,-*b*]pyrazine 6-oxide—a fused heterocycle with a roving hydrogen forms a new class of insensitive energetic materials. Chemistry 2014;20(2):542–8.
[28] Schulze MC, Scott BL, Chavez DE. A high density pyrazolo-triazine explosive (PTX). J Mater Chem A Mater Energy Sustain 2015;3(35):17963–5.
[29] Piercey DG, Chavez DE, Scott BL, Imler GH, Parrish DA. An energetic triazolo-1,2,4-triazine and its N-oxide. Angew Chem Int Ed 2016;55(49):15315–8.
[30] Tang YX, Kumar D, Shreeve JM. Balancing excellent performance and high thermal stability in a dinitropyrazole fused 1,2,3,4-tetrazine. J Am Chem Soc 2017;139(39):13684–7.
[31] Chavez DE, Parrish DA, Mitchell L, Imler GH. Azido and tetrazolo 1,2,4,5-tetrazine N-oxide. Angew Chem Int Ed 2017;56(13):3575–8.
[32] Singer IL, Pollock HM. Fundamentals of friction: macroscopic and microscopic processes. Braunlage: Springer Science+Business Media Dordrecht; 1991. p. 238–41.
[33] Dienwiebel M, Verhoeven GS, Pradeep N, Frenken JWM. Superlubricity of graphite. Phys Rev Lett 2004;92(12):126101.
[34] Lee C, Li QY, Kalb W, Liu XZ, Berger H, Carpick RW, et al. Frictional characteristics of atomically thin sheets. Science 2010;328(5974):76–80.
[35] Liu Z, Yang JR, Grey F, Liu JZ, Liu YL, Wang YB, et al. Observation of microscale superlubricity in graphite. Phys Rev Lett 2012;108(20):205503.
[36] Koren E, Lortscher E, Rawlings C, Knoll AW, Duerig U. Adhesion and friction in mesoscopic graphite contacts. Science 2015;348(6235):679–83.
[37] Zhang C. Investigation of the slide of the single layer of the 1,3,5-triamino-2,4,6-trinitrobenzene crystal: sliding potential and orientation. J Phys Chem B 2007;111(51):14295–8.
[38] Zhang C. Computational investigation on the desensitizing mechanism of graphite in explosives versus mechanical stimuli: compression and glide. J Phys Chem B 2007;111(22):6208–13.
[39] Zhang CY, Wang XC, Huang H. π-stacked interactions in explosive crystals: buffers against external mechanical stimuli. J Am Chem Soc 2008;130(26):8359–65.
[40] Ma Y, Zhang AB, Zhang CH, Jiang DJ, Zhu YQ, Zhang CY. Crystal packing of low-sensitivity and high-energy explosives. Cryst Growth Des 2014;14(9):4703–13.
[41] Zhang CY, Jiao FB, Li HZ. Crystal engineering for creating low sensitivity and highly energetic materials. Cryst Growth Des 2018;18(10):5713–26.
[42] Dong H. The development and countermeasure of high energy density materials. Chin J Energy Mater 2004;12:1–12.
[43] Deng MC, Feng YA, Zhang WQ, Qi XJ, Zhang QH. A green metal-free fused-ring initiating substance. Nat Commun 2019;10(1):1–8.
[44] Semeraro T, Mugnaini C, Manetti F, Pasquini S, Corelli F. Practical synthesis of novel purine analogues as Hsp90 inhibitors. Tetrahedron 2008;64(49):11249–55.
[45] Squarcialupi L, Falsini M, Catarzi D, Varano F, Betti M, Varani K, et al. Exploring the 2- and 5-positions of the pyrazolo[4,3-*d*]pyrimidin-7-amino scaffold to target human A1 and A2A adenosine receptors. Bioorg Med Chem 2016;24(12):2794–808.
[46] Kamlet MJ, Jacobs SJ. Chemistry of detonations. I. A simple method for calculating detonation properties of C–H–N–O explosives. J Chem Phys 1968;48(1):23–35.
[47] Kamlet MJ, Ablard JE. Chemistry of detonations. II. Buffered equilibria. J Chem Phys 1968;48(1):36–42.
[48] Kamlet MJ, Dickinson C. Chemistry of detonations. III. Evaluation of the simplified calculational method for Chapman-Jouguet detonation pressures on the basis of available experimental information. J Chem Phys 1968;48(1):43–50.
[49] Fischer D, Klapotke TM, Stierstorfer J. Potassium 1,1′-dinitramino-5,5′-bistetrazolate: a primary explosive with fast detonation and high initiation power. Angew Chem Int Ed 2014;53(31):8172–5.